

Research Article

Modeling the Environmental Hazards of El-Kharga Oasis Sand Dunes, Western Desert of Egypt, using Remote Sensing and GIS Techniques

Hanaa A. Megahed¹, Awad Hassoup², Abd El-Hay A. Farrag³, and Doaa Wahba⁴

¹Department of Geology, National Authority for Remote Sensing and Space Sciences (NARSS), Cairo, Egypt

²National Research Institute of Astronomy and Geophysics (NRIAG), Cairo, Egypt

³Department of Geology, Faculty of Science, Assuit University, Assuit, Egypt

⁴Department of Geology, Faculty of Science, New Valley University, New Valley, Egypt

Correspondence should be addressed to Hanaa A. Megahed, hanaanarss@yahoo.com

Publication Date: 19 July 2021

DOI: <https://doi.org/10.23953/cloud.ijarsg.505>

Copyright© 2021 Hanaa A. Megahed, Awad Hassoup, Abd El-Hay A. Farrag, and Doaa Wahba. This is an open access article distributed under the **Creative Commons Attribution License**, which permits unrestricted use, distribution, and reproduction in any medium, provided the original work is properly cited.

Abstract In this study, an integrated suite of Remote Sensing (RS) data and Geographic Information System (GIS) techniques supported by fieldwork is used to assess the sand dunes movement hazards at El-Kharga Oasis. Digital Elevation Model (DEM) data obtained from the Shuttle Radar Topography Mission (SRTM) and Advanced Spaceborne Thermal Emission and Reflection (ASTER) were integrated with GIS techniques to model the vulnerable locations and to study the terrain characteristics (slope angles and aspects) in the studied area. The risk assessment model output was verified with the field investigations using multi-temporal satellite images recorded between 1990 and 2019. Monthly wind roses showed that the sand drifts in the southeastern direction differed widely from one direction to another depending on the wind direction and velocity. The most important output of the spatial model's, results was a geo-hazard map that classified the sand dunes hazard zones into low, slight, moderate, and high-risk zones. It is concluded that, the sand dunes pose a serious hazard because of their fast movement and accumulation near the monumental sites, over roads and invading the agricultural fields. The obtained results can serve as a basis for planners and decision-makers to take the necessary precautions and measures to minimize the sand dune hazard's impact on the monumental sites (e.g., Hibis, El-Nadura, El-Ghueita and El-Zayyan), roads, and the agricultural fields at El-Kharga Oasis and lead to a sustainable development plan.

Keywords *Environmental Hazards; Sand Dunes Movement; Remote Sensing; Risk Assessment, Egypt*

1. Introduction

Natural hazards are spontaneously occurring physical phenomena caused by either the rapid or slow onset of the events of a geophysical, hydrological, climatological, meteorological, or biological nature, and they may be the a combination of more than one factor (IFRC, 2019 and Megahed and El Bastawesy, 2020). Sand drifting and dune movement represent one of the main potential geotechnical hazards (Al-Harathi, 2002) that affect various land use activities, particularly, the monumental sites,

cultivated lands, roads, and urban settlements (Abu Seif and El-Khashab, 2019). Sand dune structures and formations occur under desert conditions (Al-Harathi, 2002 and Megahed, 2020). The range of sand dune hazards' effects is determined by interlacing several factors including the sand dune size and type, local wind velocity, wind strength and direction, dryness degree of the environment, range of vegetation cover distribution and its density (Khedr et al., 2013).

In all global climates, sand dunes commonly have an abundant supply of incohesive sand-sized sediment ranging between 0.062 and 2.0 millimeters (mm) in diameter, strong sand-moving winds, and conditions that cause and affect sand sedimentation (Sarnthein, 1978 and Thom et al., 1994). Sand dunes are a dynamic earth surface process that arises from the Aeolian process (McKee, 1979). The grain size of sand dunes, wind speed and direction, and vegetation cover represent the main factors that obviously influence the piling of sand into dunes of particular shapes (Khedr et al., 2014). There are other factors that affect dune formation such as the obstructions to wind flow, dramatic changes in wind direction, the velocity and frequency of storms, sand availability, the thickness of sand cover, and the sudden removal of the vegetation cover. McKee (1979) categorized the sand dunes into simple, compound and complex forms. Simple sand dunes are small in most cases, a wavelength (the shortest distance from one dune crest to the other) between 10 and 500 meters (m). Another classification was established based on wind direction variability in which sand dunes are distinguished into migrating, elongating, and accumulating dunes (Wasson and Hyde, 1983; Lancaster, 1995; Thomas, 1997).

In Egypt, substantial investments have been allocated to develop El-Kharga Oasis, one of the most significant oases in the Western Desert that is currently suffering from the well-known sand dunes movement hazard (Figures 1a and 1b). In the study area, the sand dunes are classified into two major groups; crescentic and linear. Linear dunes (Figure 2a) are tall sand dunes of several meters in height, up to 250 m. In some cases, they may reach several hundreds of kilometers (desert dunes). An example is the Ghard of Abu-Muharriq. Compound crescentic dunes (Barchanoid) are the most prevalent dunes in El-Kharga Oasis, and their type and distribution are largely determined by the wind direction and velocity, the spaces between dunes, and topography. Crescentic dunes (Figure 2b) have the most dangerous effect on the environment, agriculture, and monumental sites. The menacing effects of crescentic dunes on plants include; root exposure (uprooting), plant burying due to the rapid movement of the sand dunes, and the rapid moisture loss due to the continuous sand movement, hindering and preventing the growth of vegetation cover (El-Sharaky et al., 2002). The first investigation of the sand dunes movement in El-Kharga Oasis was detected by Ashri (1973). The movement rates for 92 crescentic dunes were measured to be 12 m/yr using two aerial photographs (1944 and 1961). Embabi (1979) re-measured the rate of dune movement in El-Kharga using two topographic maps with a scale of 1:25,000 (1930, 1961). A subsequent study by Embabi (1981) revealed that the dune movement in El-Kharga was ranged between 20.8 and 100 m/yr using a set of 82 crescentic and 25 linear dunes from two aerial photographs (1961 and 1982). Issawi and El-Hinnawi (1982) reported that the rate of sand dune movement was about 30–40 m/yr at El-Kharga Oasis.

Change detection analysis includes measuring the temporal changes in land use and land cover using multi-temporal datasets (Singh, 1989; Ridd and Liu, 1998 and Darwish et al., 2020). Most change detection algorithms involve pre-classification algorithms that use simple processes such as image rationing and differencing (Singh, 1989 and Yuan et al., 1998). Post-classification methods may provide information about quantitative changes (Jensen, 2004). According to Ammar and El-Sayed (2019), dune hazard maps based on GIS and remote sensing data are required to illustrate the direction and rate of sand dune migration.

In this paper, we are strive to accurately reassess the impact of sand dune movement at El-Kharga Oasis including its movement rates, expected directions, and the potential effects on roads, cultivated lands, urban areas, and monumental sites by integrating and using of the remote sensing and GIS

analytical techniques. This comes in light of the lack of studies on the sand dune hazard assessment and their future effect on sustainable development in the study area, coupled with the fact that the early warning system information for geo-hazard parameters are often insufficient.

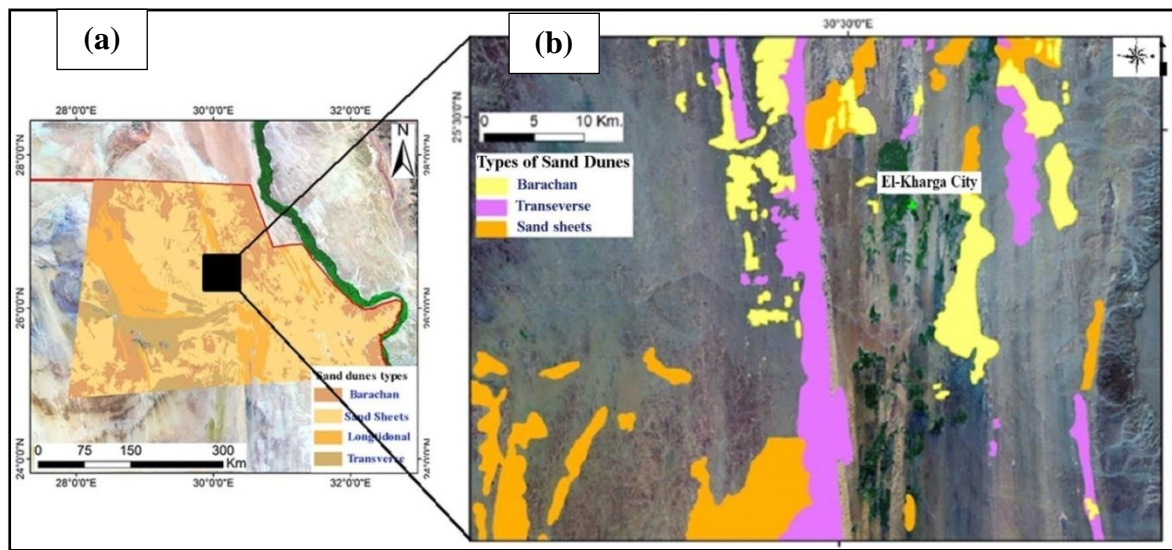


Figure 1: Landsat satellite images showing: (a) Location map of El-Kharga Oasis, Western Desert of Egypt and (b) Distribution of the sand dune fields in the study area

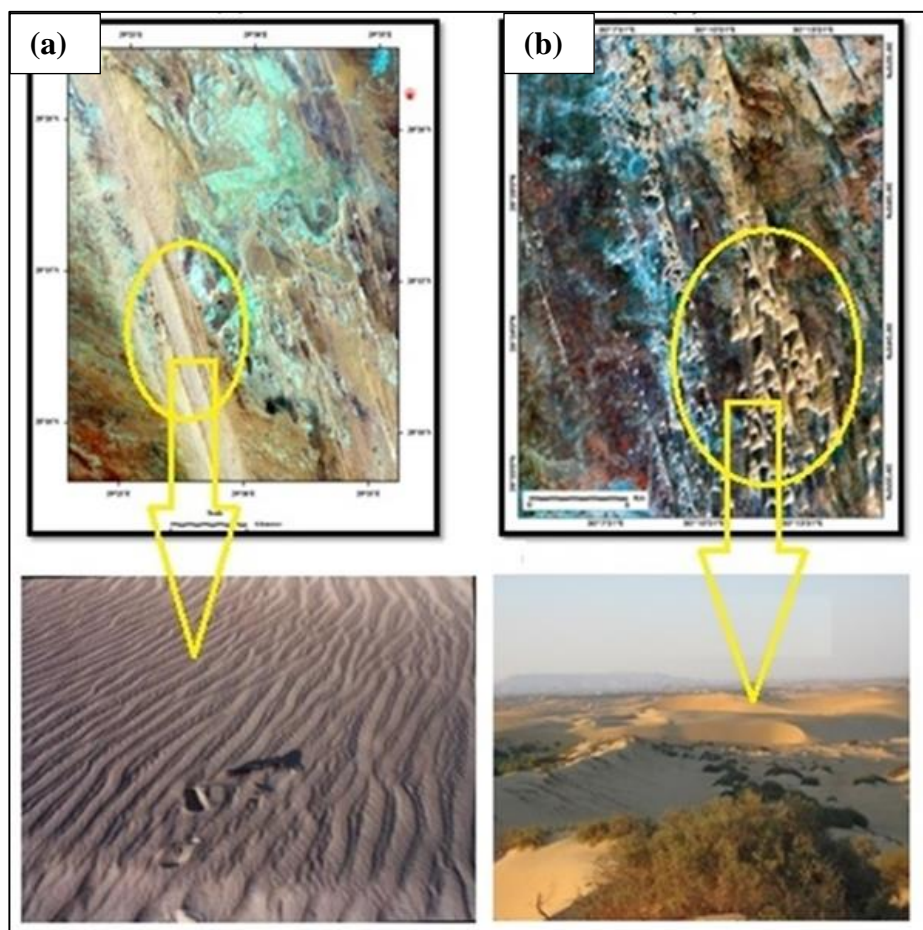


Figure 2: Field photographs and satellite images show types of dunes (a) Linear and (b) Crescentic dunes at Ghard Abu-Muharriq, El-Kharga Oasis

2. Location and geology of the study area

El-Kharga Oasis is situated at the eastern part of the Western Desert of Egypt. It forms a topographic depression of north-south orientation between latitudes $24^{\circ} 15'$ and $26^{\circ} 00'$ N, and longitude $30^{\circ} 30'$ and $30^{\circ} 45'$ E (Figures 3a and 3b).

Geologically, this depression extends southward from Abu Tartur plateau to the granitic hills of Abu Bayan. El-Kharga depression is surrounded by the Eocene limestone plateau from the east and north, with steep cliffs forming a sharp boundary that reaches the depression floor (El-Sharaky et al., 2002). The eastern plateau extends eastward to the Nile Valley with an elevation of up to 550 m (a. s. l.) and about 400 m above the depression floor (Salman et al., 2010). It is almost flat and covered by the limestone of the Lower Eocene period (Thebes Formation) (Conoco, 1987). The northern plateau rises about of 450 m above sea level (a. s. l.) at the Ain-Amor scarp. This plateau stretches northward and is covered by the limestone of the Paleocene age (Figure 4). The most prominent feature of this plateau is the absence of well-marked external drainage lines and the presence of sinkholes of various shapes (El-Shazly et al., 1982).

Regarding the climatic conditions, El-Kharga Oasis is the driest area in the Western Desert with a tropical arid climate, annual mean relative humidity of about 39 %, and extremely scarce rainfall of approximately 1 mm/yr (Kehl and Bronkamm, 1993). Wind speed is generally moderate and tends to be low in August; it increases gradually during the period ranged between November and January and reaches its maximum velocity from March to May, causing the famous “El-Khamasin” dust storms” (Salman et al., 2010).

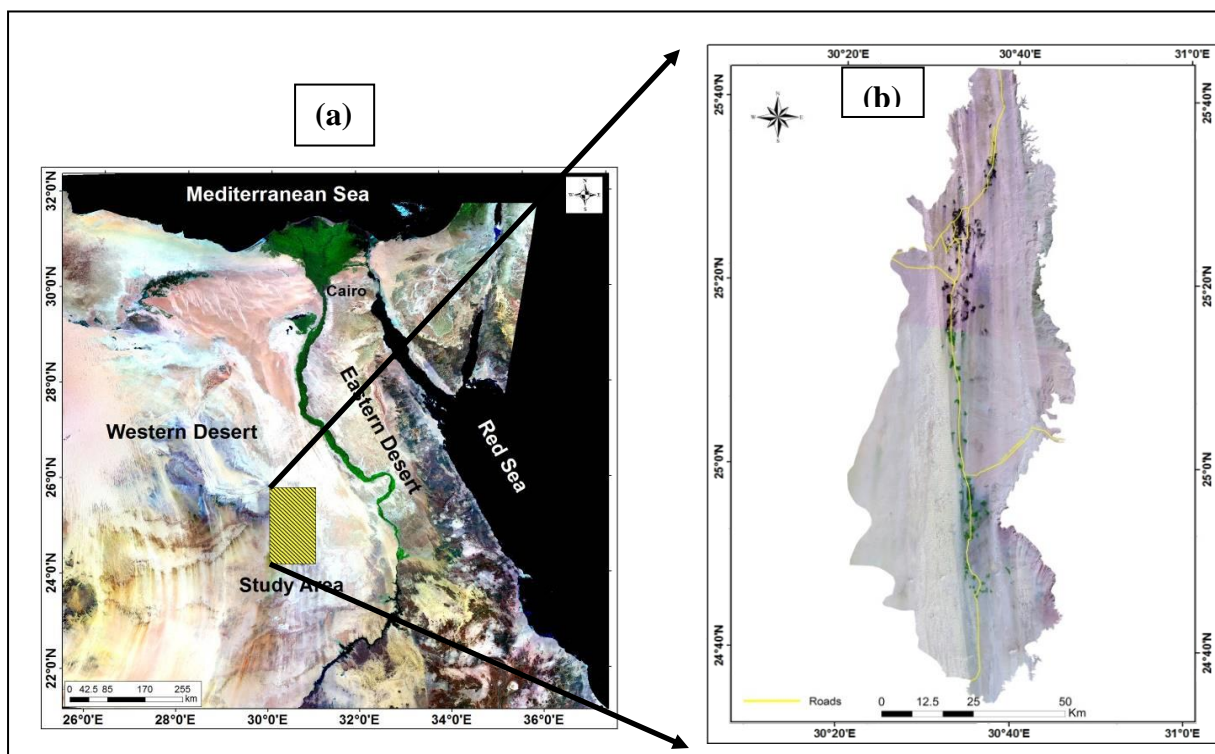


Figure 3(a) El-Kharga Oasis boundary on the satellite image of Egypt and **(b)** Landsat satellite image of the study area (May, 2019)

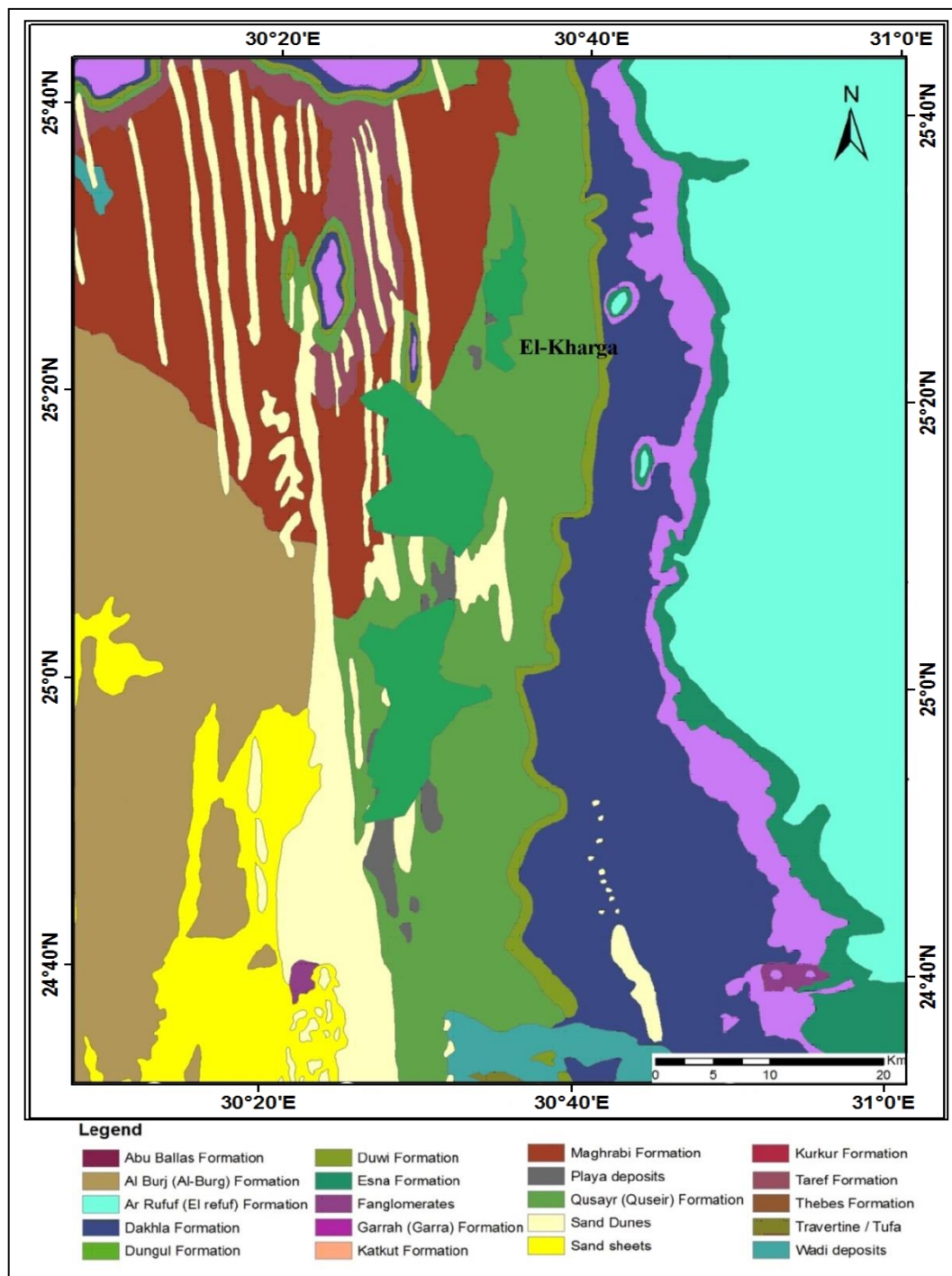


Figure 4: Geological map of El-Kharga Oasis, scale 1:250, 000, (modified, after Conoco, 1987)

3. Methodology

3.1. Dataset

Data were collected from different sources using fieldwork and processed data for integration into a GIS including; multi-temporal satellite images, a DEM, contour maps, and wind speed and direction from meteorological stations at El-Kharga Oasis. In this study, Thematic Mapper (TM) and Enhanced Thematic Mapper Plus (ETM+) images were acquired during 1990 and 2019, which were downloaded from the United States Geological Survey (USGS) database (Figures 5a and 5b). The images were rectified using ground control points.

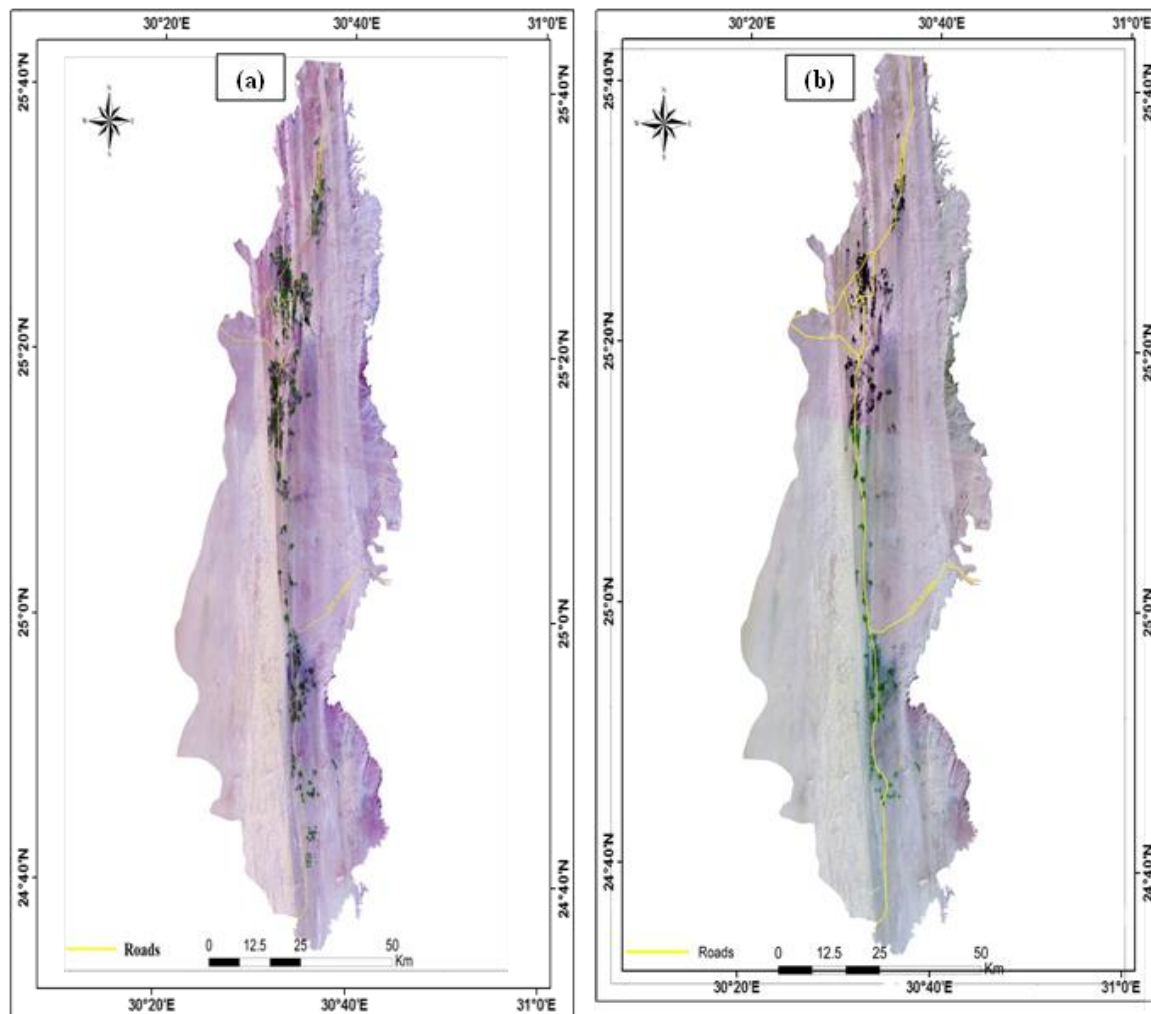


Figure 5 (a) Landsat TM image, Bands (RGB 7,4&2), (Acquisition date: May, 1990) and (b) Landsat ETM+ image, Bands (RGB 7,4&2), (Acquisition date: May, 2019)

3.2. Image pre-processing

The pre-processing steps for the Landsat images recorded from 1990 and 2019 include the various procedures needed to eliminate the radiometric, the geometric error, and the image subtraction and enhancement using Erdas Imagine 9.3 (Schiek, 2004). The aim of enhancement and subtraction of images is to improve their visual interpretability by enhancing the obvious distinction between features and making the sand dunes easier to distinguish using the percentage linear contrast stretch technique (Stow, 1999). The clip function was used for sub-setting in the Arc GIS program 10.1 (ESRI, 2014) to cover the study area.

3.3. Image post-processing

The third step was processing the digital images, which were comprised of statistical features, characteristics, and information. Processing included image classification, change detection analysis and environmental impact assessment (Xingping, 2009; Farrag et al., 2019 and Megahed, 2020). Satellite images were enhanced, analyzed, and interpreted in two steps. First, supervising the image classification performed using the maximum likelihood classifier method. The resulting classified images were then refined to illustrate the inaccurately classified pixels and increase the overall accuracy of the resulting sand dunes map. The study of change detection includes the ability to measure the temporary land use and the land cover changes through multi-temporal datasets.

4. Results and Discussion

4.1. Risk assessment modeling

Figure (6) shows the processes and analyses used to assess the risk of sand dunes and achieve the research objectives. Six significant variables are assigned for the analysis of surface terrain; as elevation, slope, slope direction (aspect), prevailing wind speed, and direction, which were extracted from the DEM and climatic data (Table 1). For developing and extracting the DEM, ARC GIS 10.1 software was used based on the ASTER.

a. Digital Elevation Model and Terrain data (slope and aspect)

The SRTM image was identified using point height DEM in which each color refers to a specific height (Figures 7a and 7b). We also applied the digital terrain model, as per its application in geomorphologic and hydrological studies (Moore et al., 1988; Megahed and Farrag, 2019).

Terrain data were obtained from a topographic contour map. Its analysis involved the processing and graphic simulation of the elevation data and included a demonstration of the slope and aspect maps (Figures 8a, 8b and 8c). The three-dimensional (3D) analysis of the Arc Map function was used to calculate the slopes in degrees and aspect angles that were also measured in degrees, with the convention of 0 degrees to the north and angles increasing clockwise. The slope and aspect were determined here for the horizontal plane. In addition, the digital elevation and digital terrain models both indicated that the study area has low relief, with the ground elevation ranging from 0 m in the northwestern part to over 364 m above sea level.

Table 1: Parameters for mapping the sand dunes movement risk.

Parameter	Parameter contributes to sand dunes activity
Digital Elevation Model (DEM)	Higher elevation zones are subjected more to the effects of the wind.
Slope angle	Steeper slope angles are riskier.
Aspect	Dune aspects facing the prevalent wind direction are more subjected to their effects.
Prevailing wind speed	Wind speed plays a crucial role in sand dunes activity
Prevailing wind direction	Prevalent wind directions affect sand dunes most.

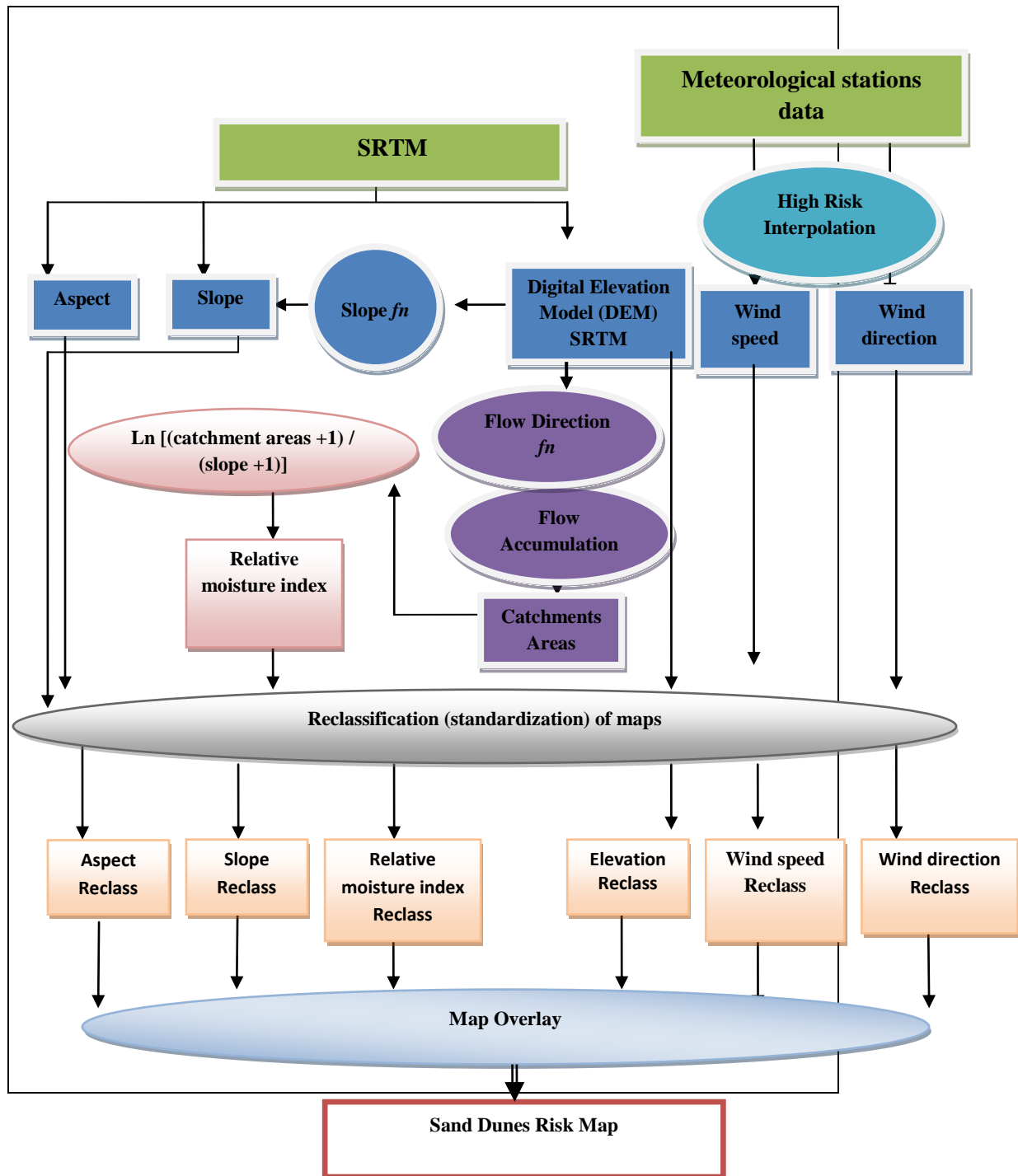


Figure 6: Flow chart of the methodology

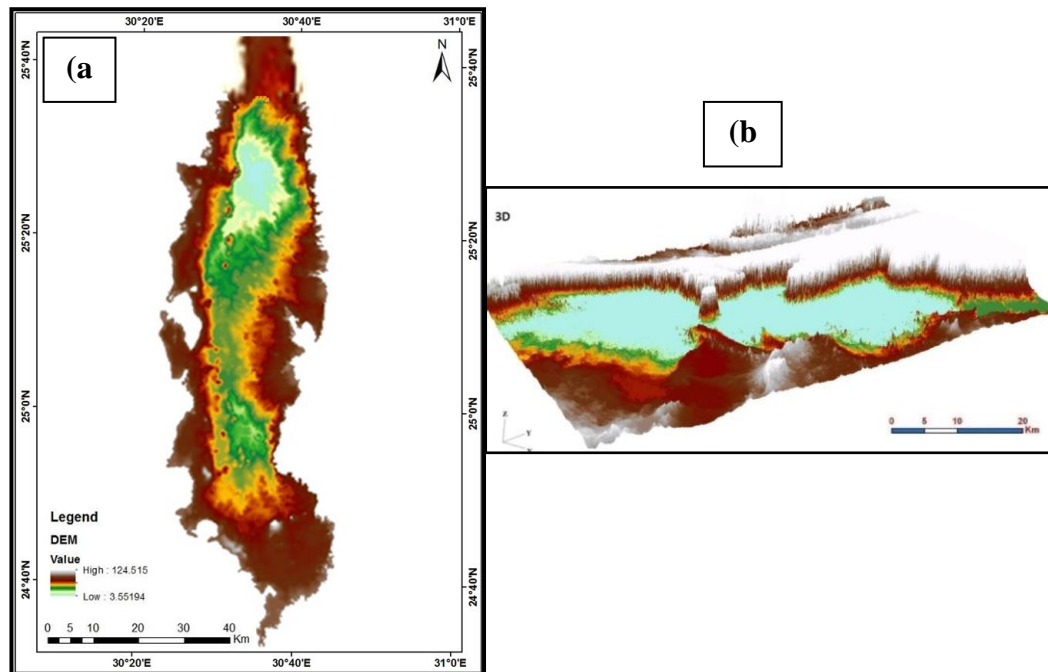


Figure 7 (a) Digital Elevation Model (DEM), extracted from the SRTM and **(b)** The 3D view of the DEM of the study area

b. Wind speed and direction

Regarding the wind speed and direction (Figure 9); in the winter, the winds move north and northwesterly in the northern part of El-Kharga Oasis, unlike in the southern part, which is dominated by south to southeasterly winds. Wind intensity is the highest in the northern part, with average speeds of 15-25 km/h that may exceed 32 km/h. The wind speed is relatively low in the southeast of El-Kharga Oasis, where quiet winds prevail from 5 to 13 km/h and increase on the western side. The winter of 2019 wind was the lowest for the past two years, with winds exceeding 24 km/h that markedly less severe wind at an average of 24-32 km/h (Egyptian Meteorological Authority, 2019) (Figure 10a). In the spring (Figure 10b), the wind direction is slightly different, as the northwest wind speeds eastward exceeding approximately 32 km/h. In the summer, the northern wind prevails in the north of the oasis, which prevails at average speeds not very different from those of the same places in the previous seasons (Figure 10c). In autumn (Figure 10d), the wind grows southwest of the oasis with speeds up to ~ 25 km/h in the north. Overall, the majority of the wind in the northern part of this area is either north or northwesterly with an average velocity of 15-25 km/h. In the south, the wind blows southeast and southwest at different intervals during the year, with speeds of < 8-18 km/h.

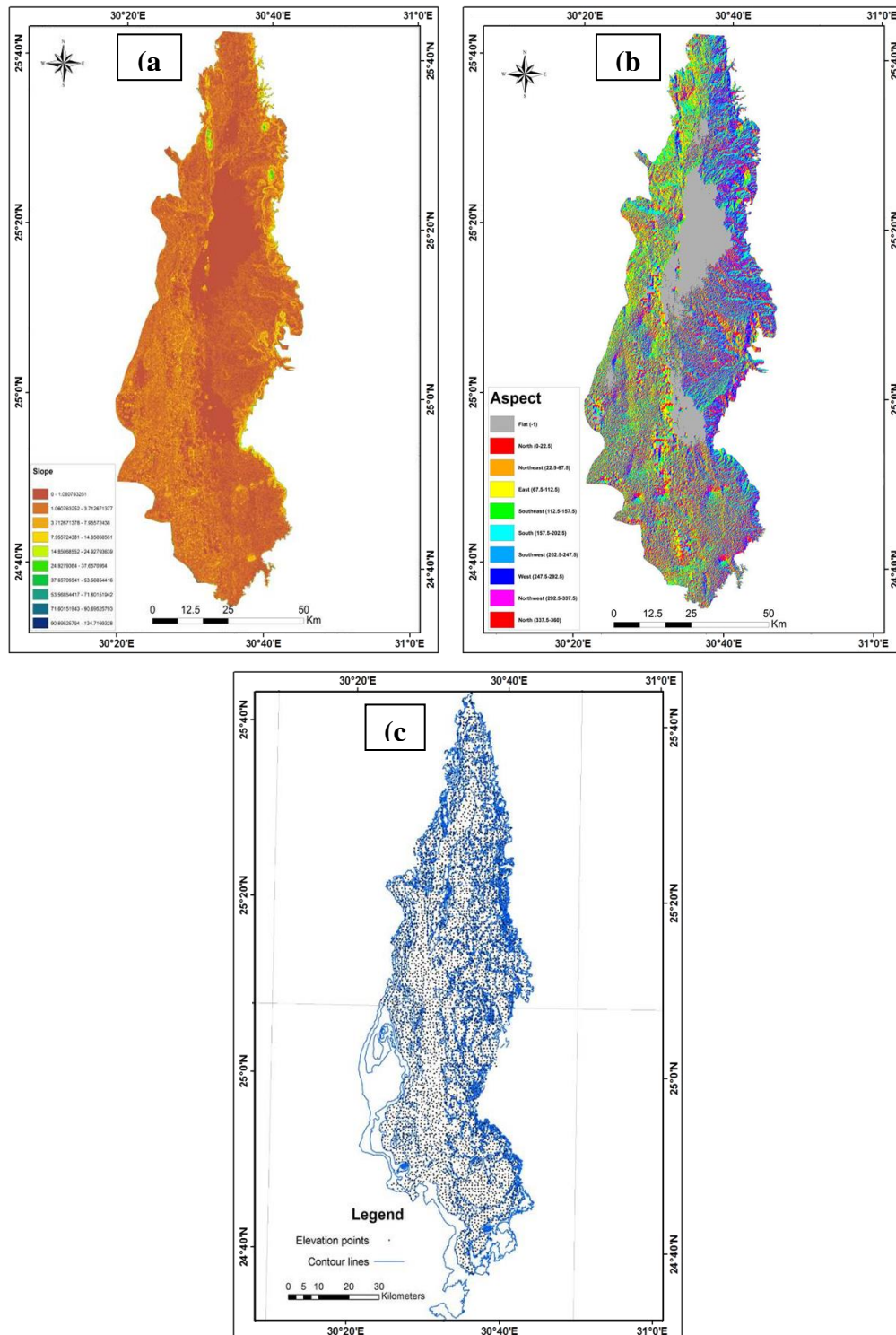


Figure 8 (a) Slope and (b) Aspect maps, extracted from (c) Contour maps of the study area

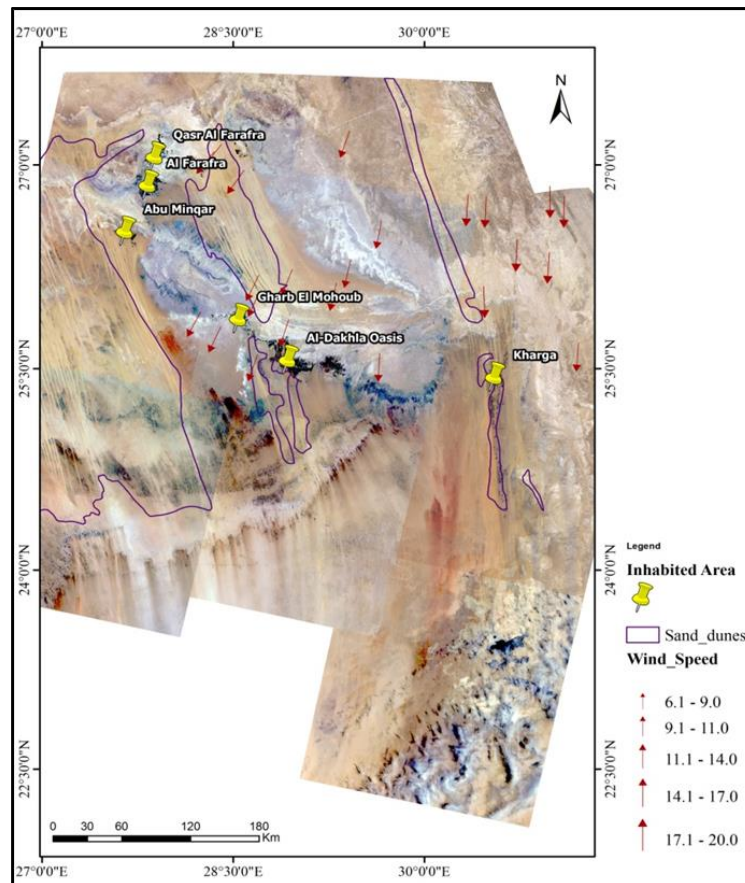


Figure 9: Wind speed data and their directions in the El -Kharga area, from the Egyptian Meteorological Authority, 2019

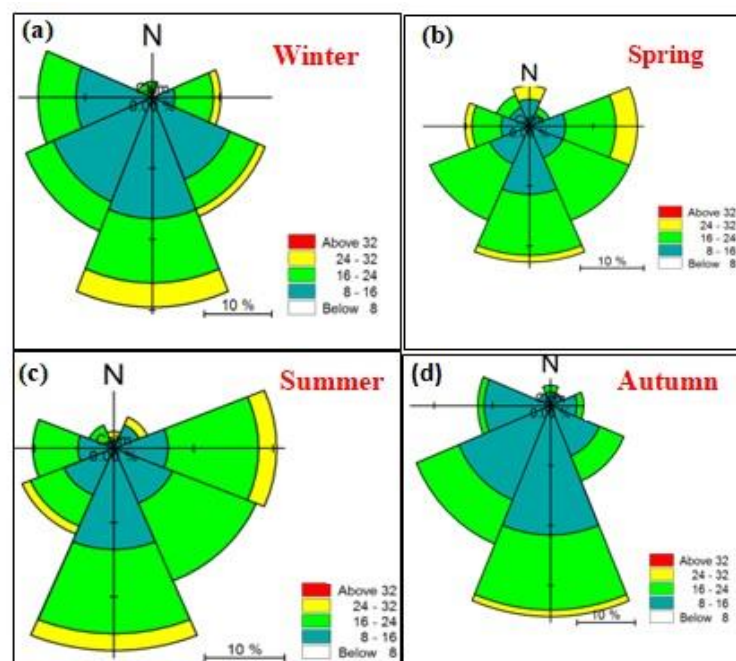


Figure 10: Wind rose diagrams showing wind the speed averages and direction in the study area during the four seasons over the two years (1990 and 2019) (a–d)

c. Sand dune speed and direction

Image classification in the present study resulted in two sand dune maps in which the spatial distribution of the dune layers for the years 1990 and 2019 are shown in Figures 11 and 12. Accordingly, 10 of the most active sand dunes in the area were chosen to represent maps identifying the changes that occurred in the dune movement during the 1990 - 2019 periods. Change detection mapping in the present study (Figure 13) clarified that the sand dunes move in the direction of the southeast, where they are affected by the speed and direction of the prevailing winds in the study area.

Heywood et al. (2002) used an advanced method of GIS analysis to introduce spatial modeling, which included the data pre-processing and a graphical representation of the modeling process as a flowchart (Figure 14). The five variables mentioned comprise the five layers of the input data (i.e., DEM, slope, aspect, prevailing wind speed, and direction) fed into a spatial model in Arc GIS 9.2 software using a weighted overlay module. All of the input grids of the weighted overlay modules are integer values. A floating-point raster was initially converted into an integer raster before using a weighted overlay module. A risk assessment map for the sand dune movement may be developed by reclassifying the parameters of the aforementioned spatial model. Based on the obtained results, the data show that the geo-hazard map presented here facilitates the classification of sand dunes hazard zone into safe, low, moderate, and high-risk zones (Figure 15).

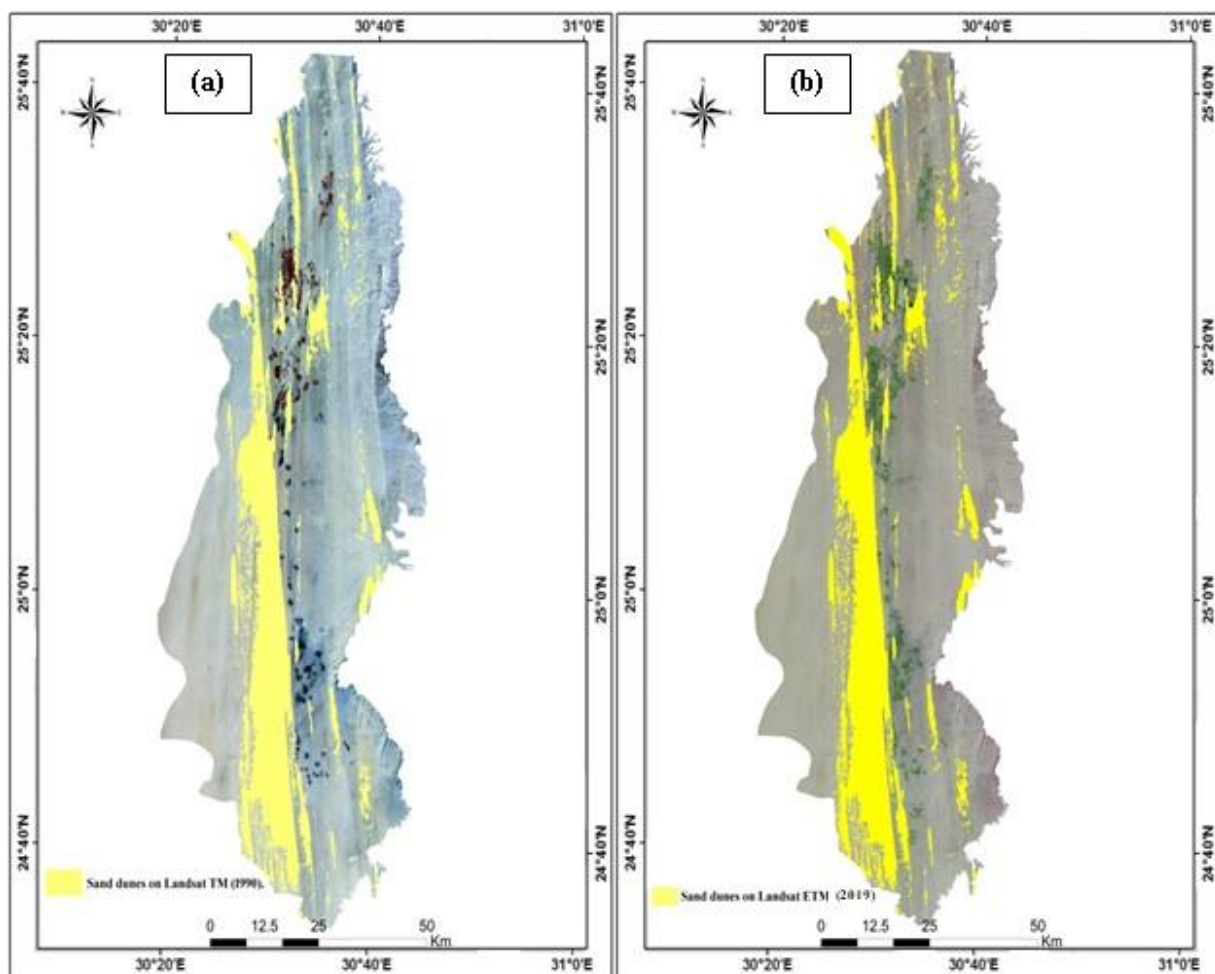


Figure 11: Sand dune layers on (a) Landsat TM image, Bands (RGB 7,4,2), (Acquisition date: May, 1990) and (b) Landsat ETM+ image, Bands (RGB 7,4,2), (Acquisition date: May, 2019)

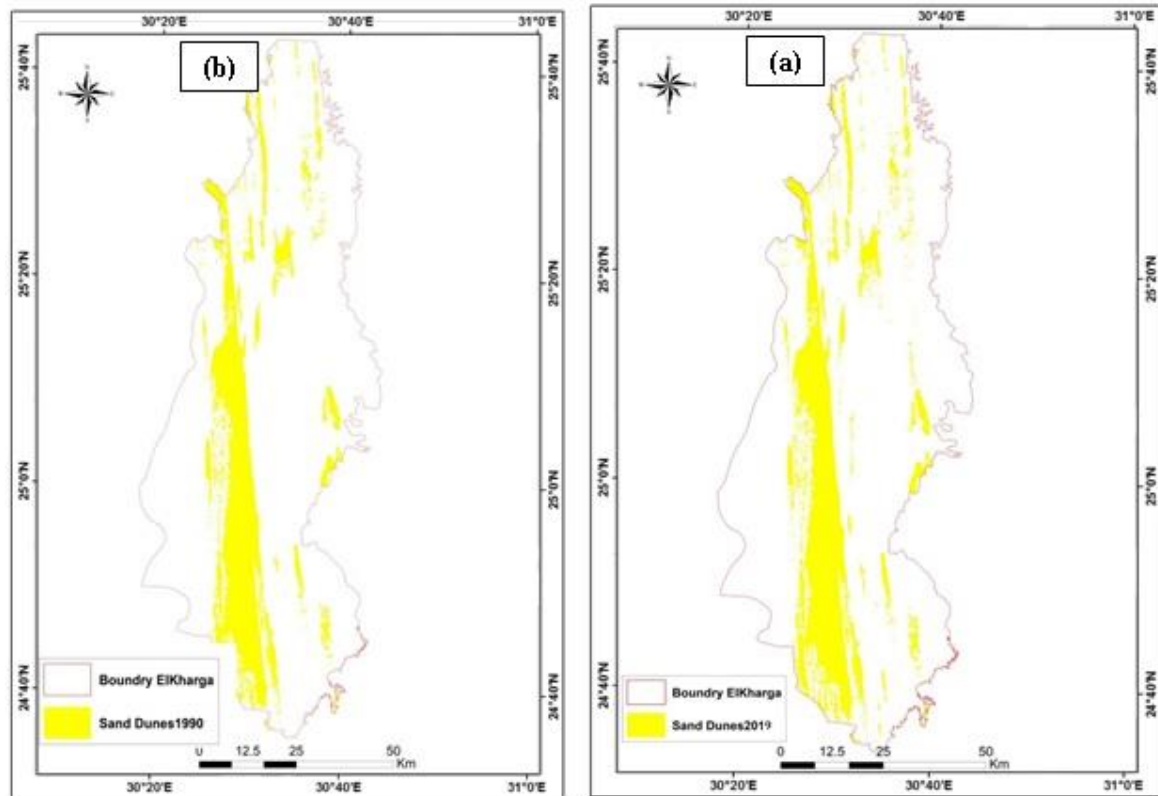


Figure 12: Sand dune movement map after reclassifying from (a) Landsat TM, (Acquisition date: May, 1990) and (b) Landsat ETM+, (Acquisition date: May, 2019)

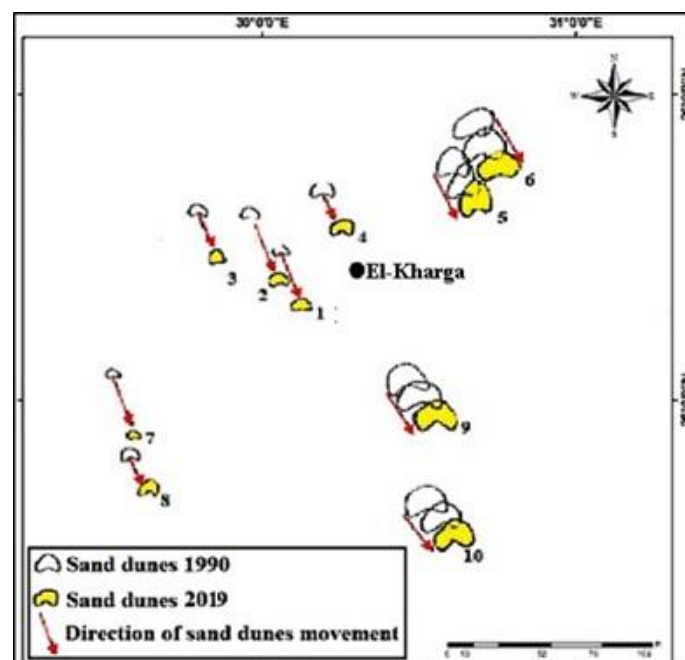


Figure 13: Change detection of 10 active sand dunes showing the rate and direction of these dunes between 1990 and 2019

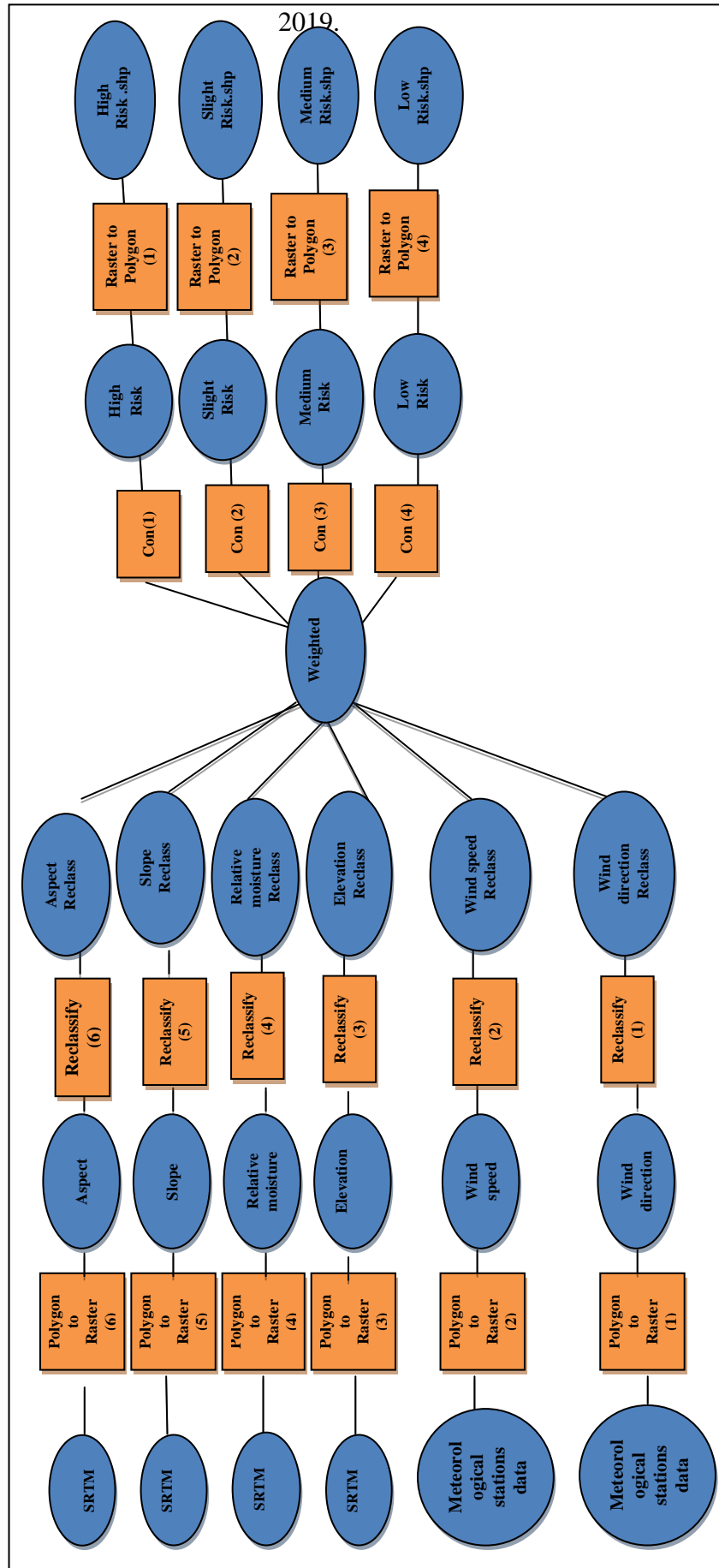


Figure 14: Spatial model framework for the sand dunes risk assessment of the study area using the Arc GIS10.1 software

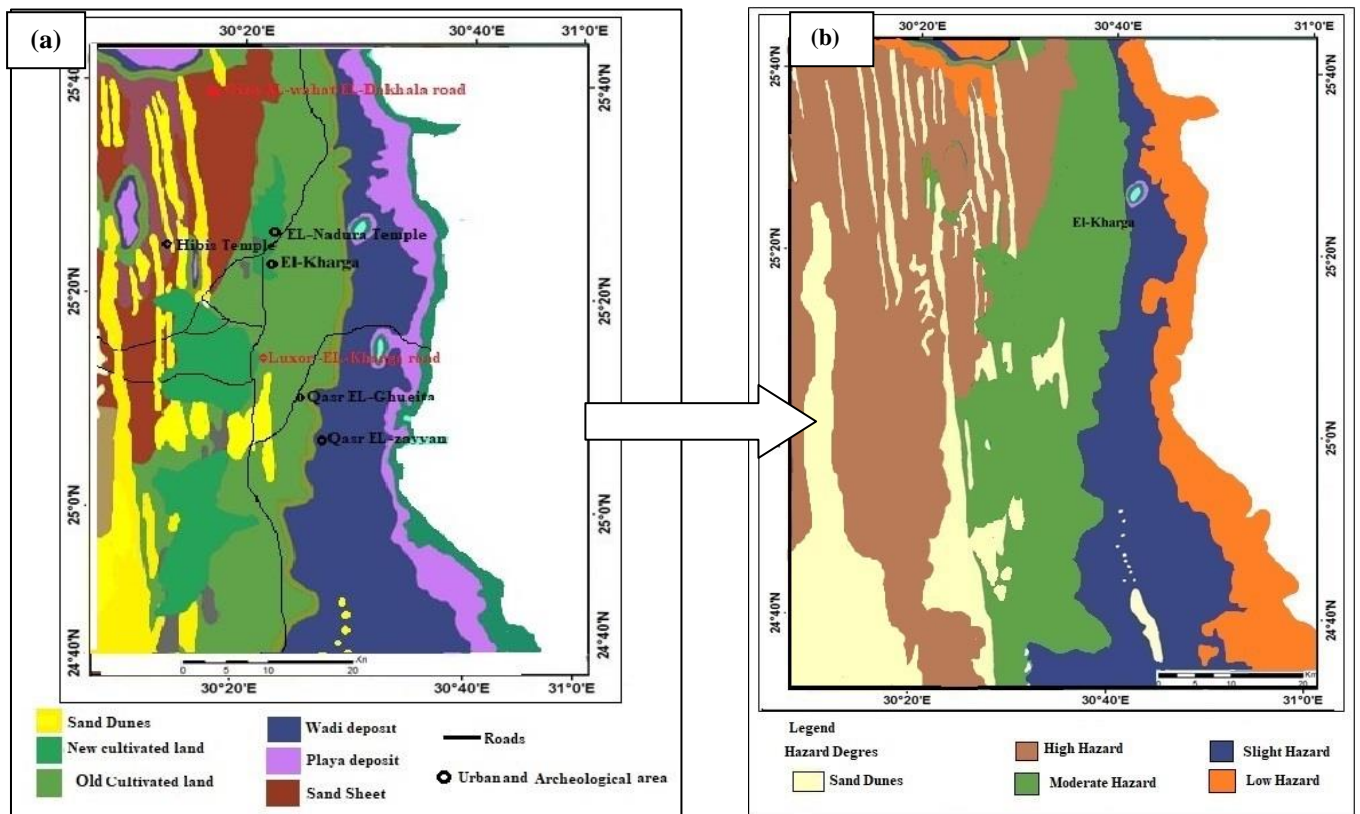


Figure 15 (a) Land use/ land cover map produced from the Landsat 8 satellite images, 2019 and **(b)** Risk assessment map showing the impact of sand dune movement on urban, cultivated, and archeological areas in the El-Kharga area

5. Conclusions and recommendations

A combination of the remote sensing and GIS techniques were applied to assess the sand dune hazards at El-Kharga Oasis in the Western Desert of Egypt. Sand dune movements have caused damage to some monuments, such as El-Nadura during windstorms. El-Ghueita Temple is another monument partially buried by strong sand dunes. The destructive elements of the sand dunes will eventually deform quite a large area of temple and monument sites in El-Kharga Oasis. Villages in El-Kharga suffer from sand dune migrations, which attack cultivated lands, water wells, and irrigating canals; as well as roads and houses. The western parts of the El-Kharga dune belt regularly threaten the El-Dakhla-El-Kharga highway after every windstorm. Dune movements attack roads in El-Kharga and the Western Desert of Egypt. El- Kharga-Assiut and El- Kharga - El- Dakhla highways are also facing sand dune encroachment (Figures 6a-f respectively). Sand dune movement hazards can be avoided by planting trees, constructing groundwater wells to irrigate trees, and making fences or barriers around the agricultural land and monumental sites, (see Figures 17a-d, respectively). The present integrative approach described in this case study will be of interest to sand dune hazard management in similar arid environments. Finally, additional studies on wind and dune movement rates and the factors that control dune movement and accumulation are required.

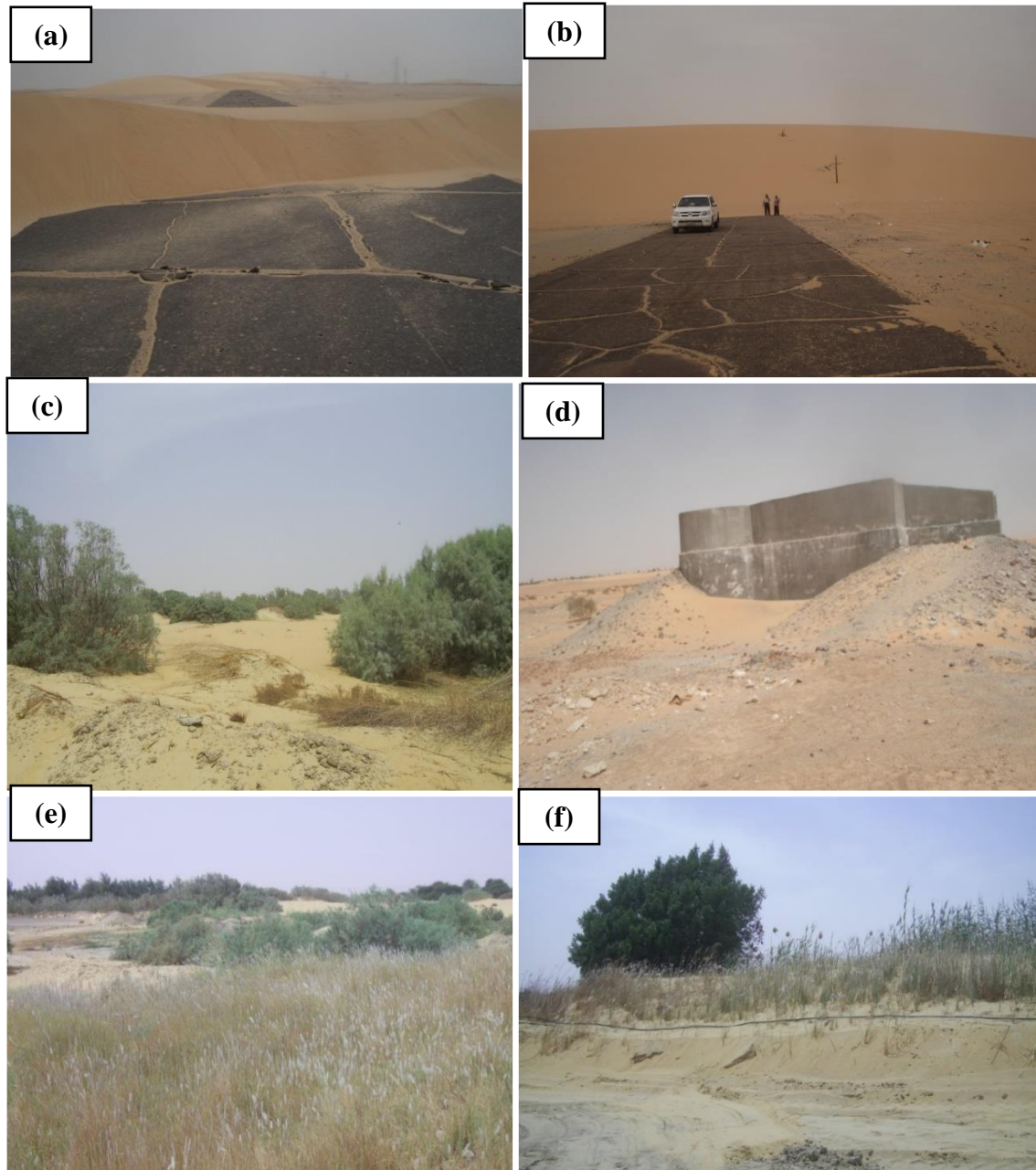


Figure 16: Field photographs showing sand dunes in 2019 (a, b) covering the El-Dakhla-El-Kharga road, (c) covering water wells, (d) sand accumulation below the northern walls of El-Nadura temple and El-Ghaueita Temple, and (e, f) sand dunes covering some agricultural areas

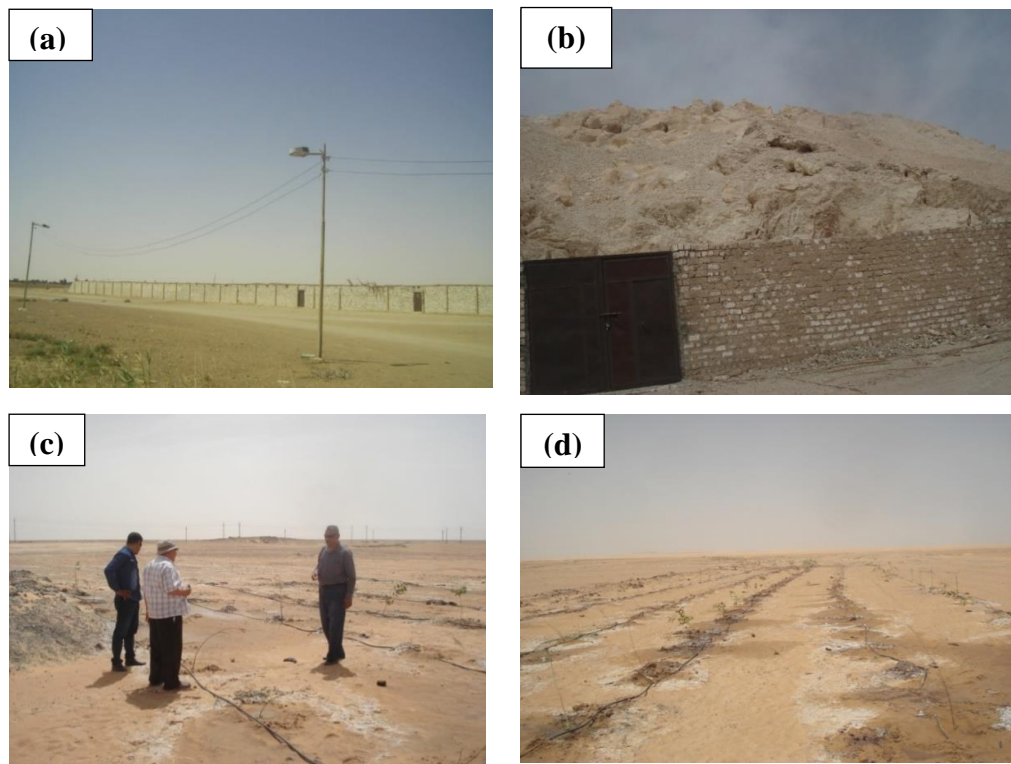


Figure 17: Field photographs in 2019 showing some actions taken in the study area to reduce sand dune movement hazards such as (a, b) fences or barriers around villages, agricultural lands and monumental sites, and (c, d) tree planting and groundwater wells construction to irrigate trees

References

- Abu Seif, E.S., El-Khashab, M.H. 2019. Desertification risk assessment of sand dunes in middle Egypt: a geotechnical environmental study. *Arab J Sci Eng.*, 44, pp.357–375. <https://doi.org/10.1007/s13369-018-3343-7>
- Al-Harathi, A. 2002. Geohazard assessment of sand dunes between Jeddah and Al-Lith, western Saudi Arabia. *Environmental Geology*, 42(4), pp.360-369. <https://doi.org/10.1007/s00254-001-0501-z>
- Ammar, A., El-Sayed, S.S. 2019. Environmental Hazards of Sand Dunes, South Jeddah, Saudi Arabia: An Assessment and Mitigation Geotechnical Study. *Earth Syst Environ*, 3, pp.173–188. <https://doi.org/10.1007/s41748-019-00100-5>.
- Ashri, A.H. 1973. The movement of sand dunes at Kharga oasis. *Geol. Soc. Egypt*, 17, pp.37-46.
- Conoco, C. 1987. Geological map of Egypt, scale 1: 500,000. Geological Survey and Egyptian General Petroleum Corporation, Cairo.
- Darwish, M.H., Megahed, H.A., Farrag, A.EH.A. et al. 2020. Geo-Environmental Changes and Their Impact on the Development of the Limestone Plateau, West of Assiut, Egypt. *Journal of the Indian Society of Remote Sensing*, 48, pp.1705–1727. <https://doi.org/10.1007/s12524-020-01158-9>
- Egyptian Meteorological Authority. 2019. The normal for El-Kharga oasis station, (1999-2019), Ministry of Civil Aviation, Cairo, Egypt.

El-Sharaky, A.M., Labib, T.M., Philip, G. 2002. Sand dune movement and its effect on cultivated lands in Africa: case study: Dakhla Oasis, Western Desert, Egypt. *Land Degradation in Egypt and Africa* (23–24 March 2002), Cairo University, pp.1-15.

El-Shazly, E.M., Abdel Hady, M.A., El-Ghawaby, M.A., Salman, A.B., El-Kassas, I.A., Khawasik, S.M., El-Amin, H., El-Rakaiby, M.M., El-Aassy, I.E., Issawi, B., El-Hinnawi, M.H. 1982. *Kharga Oasis: A Case Study*. Remote Sensing Center, Cairo, Egypt, p.31.

ESRI. 2014. Arc Map version 10.1. User Manual, 380 New York Street, Redlands, California, 92373-8100, USA.

Embabi, N.S. 1979. Barchan dune movement and its effect on economic development of the Kharga oasis depression, (in Arabic): *Jour. Middle East*, The Middle East Research Center, Ain Sams University, 6, pp.51-84.

Embabi, N.S. 1981. Barchans of the Kharga depression. *Ann. Geol. Surv. Egypt*, 11, pp.141-155.

Farage, A.E.A., Megahed, H. A., Darwish, H. D. 2019. Remote sensing, GIS and chemical analysis for assessment of environmental impacts on rising of groundwater around Kima Company, Aswan, Egypt. *Bulletin of the National Research Centre* 43, pp.14. <https://doi.org/10.1186/s42269-019-0056-3>

Heywood, I., Cornelius, S., Carver, S. 2002. *An introduction to geographical information systems*. Prentice Hall, Harlow.

IFRC, 2019. Types of disasters: Definition of hazard”, IFRC, viewed October 14, 2019, <https://www.ifrc.org/en/what-we-do/disaster-management/about-disasters/definition-of-hazard/>.

Issawi, B., El-Hinnawi, M.H. 1982. *Kharga Oasis: A Case Study*. Remote Sensing Center, Cairo, Egypt, 31p.

Jensen, J.R. 2004. Digital change detection. *Introductory digital image processing - A remote sensing perspective*, Pearson Prentice Hall, Upper Saddle River, NJ, pp.467-494.

Kehl, H., Bronkamm, R. 1993. Landscape ecology and vegetation units of the Western Desert of Egypt. In: Meissner, B., Wycisk, P. (Eds.). *Geopotential and Ecology – Analysis of a Desert Region*. Catena Supplement 26, pp.155–178.

Khedr, E., Abou Elmagd, K., Halfawy, M. 2014. Rate and Budget of Blown Sand Movement along the Western Bank of Lake Nasser, Southern Egypt. *Arabian Journal of Geosciences*, 7, pp.3441–3453. DOI10.1007/s12517-013-1006-2.

Khedr, E., Abou Elmagd, K., Halfawy, M. 2013. Factor Analysis of Meteorological and Granulometrical Data of Aeolian Sands in Arid Area as a Geo-Environmental Clue: A Case Study from Western Bank of Lake Nasser, Egypt. *International Journal of Civil & Environmental Engineering*, 13(3), pp.21-37.

Lancaster, N. 1995. Dune morphology and morphometry. *Geomorphology of desert dunes*. Routledge, London and New York. https://doi.org/10.1007/978-94-015-8254-4_18

McKee, E. 1979. Sedimentary structures in dunes. In: McKee E (ed) *a study of global sand seas*. US Geol Surv Prof Pap 1052, pp.83–133. <https://doi.org/10.3133/pp1052>

Megahed, H.A. 2020. GIS-based assessment of groundwater quality and suitability for drinking and irrigation purposes in the outlet and central parts of Wadi El-Assiuti, Assiut Governorate, Egypt. *Bull Natl Res Cent*, 44, p.187. <https://doi.org/10.1186/s42269-020-00428-3>

Megahed, H.A. 2020. Hydrological and archaeological studies to detect the deterioration of Edfu temple in Upper Egypt due to environmental changes during the last five decades. *SN Appl. Sci.*, 2, p. 1952. <https://doi.org/10.1007/s42452-020-03560-x>

Megahed, H.A., El Bastawesy, M.A. 2020. Hydrological problems of flash floods and the encroachment of wastewater affecting the urban areas in Greater Cairo, Egypt, using remote sensing and GIS techniques. *Bull Natl Res Cent*, 44, p.188. <https://doi.org/10.1186/s42269-020-00442-5>

Megahed, H.A., Farrag, A.E.A. 2019. Groundwater potentiality and evaluation in the Egyptian Nile Valley: case study from Assiut Governorate using hydrochemical, bacteriological approach, and GIS Techniques. *Bulletin of the National Research Centre*, 43, p.48. <https://doi.org/10.1186/s42269-019-0091-0>

Moore, I.D., O'Loughlin, E.M., Burch, G.J. 1988. A contour-based topographic model for hydrological and ecological applications. *Earth Surface Processes and Landforms*, 13, p.305-320. <https://doi.org/10.1002/esp.3290130404>

Ridd, M.K., Liu, J. 1998. A comparison of four algorithms for change detection in an urban environment. *Remote Sensing of Environment*, 63, pp.95-100. [https://doi.org/10.1016/s0034-4257\(97\)00112-0](https://doi.org/10.1016/s0034-4257(97)00112-0)

Salman, A.B., Howari, F.M, El-Sankary, M.M., Wali, A.M., Saleh, M.M. 2010. Environmental impact and natural hazards on Kharga Oasis monumental sites, Western Desert of Egypt. *Journal of African Earth Sciences*, 58(2), pp.341-353. <https://doi.org/10.1016/j.jafrearsci.2010.03.011>

Sarnthein, M. 1978. Sand deserts during glacial maximum and climatic optimum. *Nature*, 272(5648), p.43. <https://doi.org/10.1038/272043a0>

Schiek, G.C. 2004. Terrain change detection using aster optical satellite imagery along the Kunlun Fault, Tibet. Unpublished Ph.D. Thesis, Department of the Geological Sciences, the University of Texas El Paso.

Singh, A. 1989. Digital change detection techniques using remotely sensed data. *Int. J. Remote Sensing*, 10(6), pp.989-1003. <https://doi.org/10.1080/01431168908903939>

Stow, D.A. 1999. Reducing mis-registration effects for pixel-level analysis of land cover change. *International Journal of Remote Sensing*, 20, pp.2477–2483. <https://doi.org/10.1080/014311699212137>

Thom, B., Hesp, P., Bryant, E. 1994. Last glacial “coastal” dunes in Eastern Australia and implications for landscape stability during the Last Glacial Maximum. *Palaeogeography, Palaeoclimatology, Palaeoecology*, 111(3-4), pp.229-248. [https://doi.org/10.1016/0031-0182\(94\)90065-5](https://doi.org/10.1016/0031-0182(94)90065-5)

Thomas, D.S.G. 1997. Arid Zone Geomorphology, ed. by DSG Thomas. p.373. <https://doi.org/10.1038/304337a0>

Wasson, R.J. and Hyde, R. 1983. Factors determining desert dune type. *Nature*, 304(5924), p.337.

Xingping Wen and Xiaofeng Yang. A new change detection method for two remote sensing images based on spectral matching," 2009 International Conference on Industrial Mechatronics and Automation, 2009, pp.89-92, doi: 10.1109/ICIMA.2009.5156567

Yuan, F., Sawaya, K.E., Loeffelholz, B.C. and Bauer, M.E. 2005. Land covers classification and change analysis of the Twin Cities (Minnesota) Metropolitan Area by multi-temporal Landsat remote sensing. *Remote Sensing of Environment*, 98, pp.317-332. <https://doi.org/10.1016/j.rse.2005.08.006>